Transparent and conductive polysiloxanes/ PEDOT:PSS nanocomposite thin films with a “water-impermeable” property to significantly enhance stability of organic–inorganic hybrid solar cells

WANG, Heming and KUMAR, Vikas

Transparent and conductive polysiloxanes/PEDOT:PSS nanocomposite thin films with a "water-impermeable" property to significantly enhance stability of organic-inorganic hybrid solar cells

Heming Wang*, Vikas Kumar

Materials & Engineering Research Institute, Sheffield Hallam University, City Campus, Howard Street, Sheffield, S1 1WB, UK.

*Email: h.wang@shu.ac.uk.

Abstract: We demonstrated for the first time that optically transparent and conductive polysiloxanes/PEDOT:PSS nanocomposite thin films were produced at 85^{o}C by mixing a sol-gel modified polysiloxanes with the aqueous PEDOT:PSS solution. Polysiloxanes/PEDOT:PSS nanocomposite thin films were deposited by conventional solution-processed spin- or spray-coating methods, presenting superior water- and scratch-resistance. ~100 Ω/□ sheet resistance with ~ 80% transmittance was obtained and was further reduced to 25 Ω/□ by adding 90 nm±20 nm Ag nanowires in the solution. The p-type polysiloxanes/PEDOT:PSS nanocomposite thin films were then applied on n-type c-Si wafers to fabricate organic-inorganic Schottky hybrid photovoltaic devices, demonstrating the similar performance in power conversion efficiency as PEDOT:PSS. However, To the best of our knowledge our high conductive polysiloxanes/PEDOT:PSS nanocomposite c-Si hybrid photovoltaic devices presented the best stability among this type of devices under the ambient environment. Performance of our photovoltaic devices kept no degradation even if the devices were immersed in water without encapsulation for protection.

Keywords: transparent and conductive coatings, organic-inorganic hybrid solar cells, polysiloxanes, sol-gel, PEDOT:PSS.

1. Introduction

Organic-inorganic hybrid photovoltaic (PV) devices have showed their promising in replacing or reducing the fabrication cost of conventional Si wafer-based p-n junction solar cells that currently dominate the PV market with over 80% of the market share. The relatively high cost of the PV modules using Si p-n junction wafer solar cells compared to conventional fossil fuels-based energy restricts its wide adoption for the civil electricity supply. Hybrid n-type c-Si/Poly(3,4-ethylenedioxythiophene):poly(styrene sulfonic acid) (PEDOT:PSS) Schottky PV devices are regarded as new generation low-cost Si-based solar cells that can potentially reduce the price of the PV modules because transparent organic conducting polymer PEDOT:PSS can be fabricated on n-type c-Si wafers using the simple solution-processed method at low temperature of ~120^{o}C. However, although high-efficiency n-type c-Si/PEDOT:PSS-based solar cells were widely reported,[1-9] they suffered from the notorious stability issues of organic-inorganic hybrid PV devices because of poor water resistance of PEDOT:PSS.[10-11] The power conversion efficiency (PCE) of PV devices will decrease seriously if stored under ambient conditions without encapsulation. Long term stability of the hybrid PV modules is one of the key factors that need to be addressed for competing with the conventional Si p-n wafer-based solar cells.[12] In this paper, for the first time we reported a novel polysiloxanes/PEDOT:PSS (PSES:PEDOT:PSS) nanocomposite thin film that was used to fabricate the n-type c-Si/PSES:PEDOT:PSS PV devices. Our hybrid PV devices presented an exceptional stability to the environment through experiments of immersing the unprotected PV devices in water, which illustrated that optically transparent and highly conductive PSES:PEDOT:PSS nanocomposite thin films presented a “water-impermeable” property.

PEDOT has potentially wide applications in optoelectronic, electronic, electrical, and electrochemical devices due to its high electrical conductivity, thermal and chemical stability,

high transparency, and low-cost.[13][14] However, co-polymer PEDOT:PSS thin films from an aqueous solution have very poor water resistance. Properties of the PEDOT:PSS film including its adhesion to the substrate are significantly affected by water or ambient environment. A phenomenon is that the PEDOT:PSS thin film disintegrates and is removed or peels off from the substrate shortly after immersion in water. Although many studies have been carried out to form composites or nanocomposite PEDOT:PSS thin films by combining either inorganic nanoparticles (NPs) or organic components,[15][16] no report demonstrated that transparent and highly conductive properties via addition of assistant solvents [17] (e.g. typically of dimethyl sulfoxide (DMSO)) and a water-proof bonding to the substrate were achieved. The doped components in the nanocomposites either reduced the conductivity of PEDOT:PSS due to percolation or provided no contributions on forming a strongly water-resistant bond to the substrate. In this report, a PSES ($[RR'SiO]_m[(SiO_4R''SiO_2]_n$) derived from a sol-gel method was able to combine with PEDOT:PSS to form optically transparent and highly conductive nanocomposite thin films. The sol-gel modified PSES provided significant water- and scratch- resistance through the chemical bonding while PEDOT:PSS delivered its electrical conductivity. The mixed solution from the PEDOT:PSS aqueous solution with the sol-gel PSES solution changed neither their easy-processable properties by the solution-based method nor the tuneable electrical conductivity via assistant solvents.

2. Experimental section

Preparation of the PSES:PEDOT:PSS solution

A hybrid sol was first prepared by the sol-gel method from precursors of tetraethyl orthosilicate and triethoxymethylsilane that were mixed in the solvent of isopropanol by dropwise adding deionised (DI) water at the mole ratio of 18:14:17:220. The sol-gel modified PSES solution was then obtained by adding 12 mole % an unknown -OH terminated polysiloxanes polymer into the hybrid sol. The PEDOT:PSS aqueous solution was obtained

by dissolving 1.0 wt % PEDOT:PSS pellets (from Sigma-Aldrich) in DI water. The PSES:PEDOT:PSS solution labelled as SGP-1 was then produced by mixing the modified PSES solution and the PEDOT:PSS aqueous solution with isopropanol at the volume ratio of 1:2:1. Similarly, the high conducting PSES:PEDOT:PSS (hcPSES:PEDOT:PSS) solution labelled as SGP-2 was obtained by replacing the PEDOT:PSS aqueous solution with the high conducting PEDOT:PSS (hcPEDOT:PSS) aqueous solution (from Sigma-Aldrich) at the same amount as that in SGP-1. 20 mg/ml Ag nanowires (with on average ~30 μm at length and 90±20 nm at diameter) dispersed in isopropanol was used to add Ag nanowires into the PSES:PEDOT:PSS solution at the volume ratio of 1:0.5. The Ag nanowires solution was also utilized for fabrication of the top contact electrode in our hybrid PV devices.

Preparation of thin films

PSES:PEDOT:PSS Thin films were casted on either polyacrylic plastics (PP) or glass slides (GS) by the spin-coating method at the rpm of 1000 or the spray-coating method. PP or GS were respectively cleaned by soap water, DI water, and isopropanol before applying the thin films. The casted thin films were subsequently cured by placing in an oven at 85^{o}C for ~30 min. Multiple-coatings were achieved by this repeated procedure.

Preparation of silicon

1-4 Ω.cm n-type Si (100) wafers from Virginia Semiconductor Inc. were cut into area of ~1.5x1.5 cm^2 and then ultrasonically cleaned with acetone, isopropanol, and DI water, separately. The cleaned samples were dried with N_2-blow and then were immersed in the 5 % HF solution for 2 min to remove the oxides on the surfaces. The treated samples were then cleaned with DI water and dried again with N_2 blow. The unpolished surface of Si substrates was deposited with Sn metal (~150 nm) using the single target magnetron sputtering system (Q150T) immediately after the HF treatment.

Fabrication of the hybrid solar cells

The controlled samples of hybrid PEDOT:PSS PV devices were fabricated using the PEDOT:PSS or hcPEDOT:PSS aqueous solution on the treated n-type Si wafers. A thin layer of PEDOT:PSS containing 10 % DMSO was spin-coated on the silicon and then heated at 130^{o}C for 10 min. Ag nanowires from the Ag nanowire isopropanol dispersion were spray-coated on top of the PEDOT:PSS layer to form the top electrode or alternatively separate high conductive silver paste dots with 1 cm distance away was created on top of the PEDOT:PSS layer instead of Ag nanowires as the top contact points for testing. Similarly, hybrid PSES:PEDOT:PSS PV devices were also produced using PSES:PEDOT:PSS plus 10% DMSO instead of the PEDOT:PSS aqueous solution. Hybrid PSES:PEDOT:PSS PV devices for the water immersion tests also used only separate silver paste dots with 1 cm distance away on top of the hcPSES:PEDOT:PSS layer as the top contact points.

Characterization

Transmittance tests were carried out by the Varian 50 Scan UV–Vis Spectrophotometer. For the sheet resistance measurement, two contacts were created by a high conductive silver paste, separated by a square area of the transparent PSES:PEDOT:PSS coating, and then the resistance was measured by the zero-calibrated multimeter. PV devices were illuminated using a solar simulator at one sun (AM 1.5, 100 mW/cm^2) and the J-V characteristics were measured by a Keithley 2400 electrometer. The scanning electron microscope (nanoSEM) at 15 kV and the tapping mode atomic force microscope (AFM) images were recorded using FEI™ Nova NanoSEM and Vecco Nanoscope III AFM, separately. Fourier transform infrared (FTIR) measurements were conducted with a Nicolet Nexue FTIR spectro-photometer.

3. Results and discussion

The PSES:PEDOT:PSS solution plus 10% DMSO was used to coat PP or GS substrates. With the evaporation of liquid from the solution, it formed an ideal nanocomposite substance as schematically shown in Figure 1 that contains a continuous solid skeleton (PSES) enclosing a continuously fluid-dispersed phases (PEDOT:PSS) in colloidal dimensions. Continuity means that one could travel through the solid phase from one side of the sample to the other without having to enter the fluid-dispersed phases; conversely, one could make the same trip entirely within the fluid-dispersed phases. This self-organised structure was achieved due to hydrophobicity of PSES, which makes them separate from PEDOT:PSS fruit phases. 1:2 ratio of PSES to PEDOT:PSS in the mixture obtained a balance with maximum electrical conductivity, best water-resistance, and strongest adhesion to the substrate. In order to realise the maximum thickness of thin films from this formulation that will provide the best "water-impermeable" property, variable thicknesses of multiple-layer thin films were obtained by the spin-coating method on PP substrates. Micro fractures on the thin films were observed until seven-layer thin films were deposited on PP. A cross-section backscattered SEM image of the six-layer thin film was illustrated in Figure 2a where the thickness of the six-layer film was approximately 24 μm. Therefore, we estimated that the thickness for each layer was ~4 μm. EDX elemental of Si and C mappings was used to confirm the PSES:PEDOT:PSS cross section film in Figure 2a. Surface morphologies of the PSES:PEDOT:PSS thin films were further investigated by both the scanning electron microscope (SEM) and the atomic force microscope (AFM) respectively. Images were presented in Figure 2b and Figure 2c where the thin films were composed of NPs with the sizes below 10 nm. PSES and PEDOT:PSS NPs were within the same range of dimensions and were well mixed together except a few slightly larger NPs that may come from the congregated PSES.

Without an addition of DMSO, nanocomposite thin films had very high sheet resistance (greater than 100 k Ω / □) similar to PEDOT:PSS. However, sheet resistance was significantly reduced by adding 10 vol.% DMSO in SGP-1 or SGP-2. Transmittance and sheet resistance of PSES:PEDOT:PSS thin films on PP were shown in Figure 3a where samples A, B, and C were produced from SGP-1 with ~4-, ~12-, and ~24-μm thicknesses, separately. They respectively presented ~10.4, ~3.4, and ~1.7 kΩ/□ sheet resistance (equivalent to ~ 0.245 S/cm) with on average ~ 98%, ~ 95%, and ~86% transmittance in the visible light wavelengths range after the baseline was corrected. We noticed that high transparency was still kept even if the thickness of the PSES:PEDOT:PSS thin film reached 24 μm. In comparison with PEDOT:PSS, this high transparency was impossible to be achieved at the same thickness. Furthermore, sheet resistance of thin films produced from SGP-2 was significantly reduced. Their relationship of sheet resistance and transmittance was illustrated in Figure 3b where sheet resistance decreased from ~181 (equivalent to ~ 2.30 S/cm) to ~ 42 Ω/□ and the corresponding transmittances reduced from ~85% to ~58%. Sheet resistance of the nanocomposte thin films can be further reduced by adding Ag nanowires (NWs) in SGP-1. As shown in Figure 3c, sheet resistance of the thin film produced by the spray-coating method on PP substrates decreased to ~25 Ω/□ with on average ~80% transmittance. The PSES:PEDOT:PSS film had the capability of not only preventing Ag NWs films from oxidation and corrosion but also providing a strong adhesion to the substrate. The Ag NWs used in this work had on average 90±20 nm at diameter and ~30 nm at length. Therefore, we expected that 85% transmittance with ~10 Ω/□ sheet resistance can potentially be obtained by optimising Ag NWs with ~35 nm at diameter.

Water and acid resistance were significantly enhanced for the PSES:PEDOT:PSS thin film. The SGP-1 or SGP-2 coated PP and/or GS samples were then immersed in DI water or 10% HCl aqueous solution for three weeks. Adhesion of the PSES:PEDOT:PSS thin film to the

substrates was measured after immersion according to ASTM D3359-09e2. A cross-hatch cutter or scribe was used to cut a lattice-like pattern with ~1.0x1.0 mm size for each separate square in the pattern on the substrate. Special sellotape was applied onto this region and then pulled off. No any sign of detachment for each square was observed from the pattern, illustrating an excellent adhesion to the substrate. Electrical conductivity presented negligible changes after the immersion test. By comparison, thin films from the aqueous PEDOT:PSS solution can immediately be removed from the substrate after immersion in water. Mechanical properties were also compared by the pencil hardness test according to ASTM Test Method D 3363. The PSES:PEDOT:PSS thin films on PP substrates showed ~ 6H pencil hardness while the PEDOT:PSS thin film had only below 4B pencil hardness, which demonstrated that the PSES has enormously increased scratch resistance of the PEDOT:PSS thin film.

Table 1 Performance parameters of PSES:PEDOT:PSS and PEDOT:PSS hybrid PV devices using the Ag paste dots as the top contact points for testing, respectively.

PV Devices	V_{oc} (V)	J_{sc} (mA/cm^2)	PCE (%)	FF (%)
PSES:PEDOT:PSS	0.40	7.93	1.32	42
PEDOT:PSS after preparation	0.40	12.54	2.81	56

The PSES:PEDOT:PSS nanocomposite thin film was subsequently applied on n-type c-Si wafers to fabricate hybrid photovoltaic (PV) devices using high conductive Ag paste dots as the top contact points for testing. Schematic diagram of the device structure was shown in Figure 4a as Sn film/c-Si/PSES:PEDOT:PSS or PEDOT:PSS/Ag paste dots. Figure 4b illustrated J-V characterisation of hybrid PV devices produced by PSES:PEDOT:PSS or

PEDOT:PSS, respectively. The hybrid PSES:PEDOT:PSS PV device presented poor performance with 1.32% power convention efficiency (PCE). All parameters from the J-V curve were listed in Table 1. The PSES:PEDOT:PSS PV device had V_{oc} of 0.40 V, short circuit current density (J_{sc}) of 7.93 mA/cm^2, and fill factor (FF) of 42%. Inferior performance of the PSES:PEDOT:PSS PV device was assigned to low conductivity (low positive charge transport) of the nanocomposite thin film (~ 0.245 S/cm) compared to that of PEDOT:PSS.[18] On the contrast, the PEDOT:PSS hybrid PV device achieved much better performance as listed in Table 1. It obtained PCE of 2.81% with V_{oc} of 0.40 V, J_{sc} of 12.54 mA/cm^2, and FF of 56%. Much higher conductivity of the PEDOT:PSS layer than that of PSES:PEDOT:PSS played a key role on securing better efficiency devices. Nevertheless, the PEDOT:PSS PV device fully degraded after stored in air for overnight as shown in Figure 4b, illustrating very poor stability.

Table 2 Performance parameters of hcPSES:PEDOT:PSS and hcPEDOT:PSS hybrid PV devices using Ag nanowires as the top contact electrode, respectively.

PV Devices	V_{oc} (V)	J_{sc} (mA/cm^2)	PCE (%)	FF (%)
hcPSES:PEDOT:PSS	0.52	17.34	4.74	53
hcPEDOT:PSS	0.48	20.41	4.63	47

The hcPSES:PEDOT:PSS nanocomposite thin films from SGP-2 were also utilised to fabricate the n-type Si-based hybrid PV devices with Ag nanowires as the top contact electrode. As a comparison, the controlled sample of n-type Si-based hybrid PV devices were simultaneously fabricated using the corresponding hcPEDOT:PSS. Device structures as shown in Figure 5a were of Sn film/c-Si/hcPSES:PEDOT:PSS or hcPEDOT:PSS/Ag NWs.

We characterised J-V behaviour of the hcPSES:PEDOT:PSS and hcPEDOT:PSS hybrid PV devices as presented in Figure 5b, respectively. Performance parameters according to J-V curves were illustrated in Table 2. A similar PCE of the PV devices from hcPSES:PEDOT:PSS as that of hcPEDOT:PSS was obtained. The PV device from hcPSES:PEDOT:PSS presented ~ 4.74% PCE compared to ~ 4.63% of the device from hcPEDOT:PSS. The hcPSES:PEDOT:PSS PV device had V_{oc} of 0.52 V, J_{sc} of 17.34 mA/cm^2 and FF of 53% while the hcPEDOT:PSS PV device showed lower V_{oc} of 0.48 V, higher J_{sc} of 20.41 mA/cm^2, and smaller FF of 47%. PCE of n-type Si-based hybrid solar cells can be affected by many factors like HF etching methods (e.g. creating Si nanowires structures for enhancing light absorption), hole conductivity of hcPSES:PEDOT:PSS or hcPEDOT:PSS, transmittance and sheet resistance of top electrode, and contact resistance of front and back electrodes. In comparison with the PEDOT:PSS PV device listed in Table 1, the hcPEDOT:PSS PV device in Figure 5b demonstrated much higher PCE. The cause was mainly due to the improved top contact electrode. Silver nanowires provided better contact and lower resistance for charge transport and hence enhanced the PCE of the PV devices. In the following paragraphs, we also demonstrated that the hcPEDOT:PSS PV device with the same structure as shown in Figure 4a obtained the similar J-V performance as the PEDOT:PSS PV device in Figure 4b. It was noticed that the hcPEDOT:PSS thin film had much higher conductivity (up to 1000 S/cm) [19] than the hcPSES:PEDOT:PSS nanocomposite thin film; Nevertheless, the hcPEDOT:PSS hybrid PV device did not obtain much better PCE than the hcPSES:PEDOT:PSS PV device. Further compared the PEDOT:PSS PV device with the PSES:PEDOT:PSS PV device in Figure 4b, the PEDOT:PSS PV device illustrated much better J-V behaviour. Therefore, we inferred that it required a critical value (or in a range of the value) of conductivity (C_k) for the p-type semiconductor layer on the n-type c-Si to fabricate high efficiency Schottky PV devices.

When conductivity of the p-type semiconductor layer is lower than C_k, J-V performance of the fabricated PV device was seriously affected by the value of conductivity; e.g. PSES:PEDOT:PSS PV devices in Figure 4b. However, when conductivity for the p-type semiconductor layer is greater than C_k, it no longer plays a key role on the J-V performance of the hybrid PV devices; e.g. hcPSES:PEDOT:PSS and hcPEDOT:PSS PV devices in Figure 5b. Another point for PSES:PEDOT:PSS PV devices is that they demonstrated the same J-V performance as the hcPEDOT:PSS PV devices but had overall a lower conductivity of the p-type semiconductor layer, which may imply that the PSES:PEDOT:PSS nanocomposite thin film has a high conductivity along the direction perpendicularly to the surface of the c-Si substrate. Further investigation is required for this.

Table 3 Performance parameters of hcPSES:PEDOT:PSS hybrid PV devices using the Ag paste dots as the top contact points for testing, respectively.

Devices	V_{oc} (V)	J_{sc} (mA/cm^2)	PCE (%)	FF (%)
Initial	0.40	10.52	1.92	46
24 hr	0.42	10.94	2.20	48
140 hr	0.44	10.87	2.32	49
96 hr immersion in H_2O	0.42	11.08	2.20	47

Overall, our PV devices referred to other published papers (10 to 13% PCE) had a relatively low PCE, which was mainly due to two factors; i.e. flat c-Si etching surface that had small light absorption compared to Si NWs surfaces and high contact resistance from the front and rear contact electrodes.[9] The objective in this work mainly focused on studies of enhancing

device stability through comparison; therefore, we did not adopt the best device structure in our experiments for obtaining high efficiency. Conversely, the device structure, Sn film/c-Si/PSES:PEDOT:PSS or PEDOT:PSS/Ag paste dots as shown in Figure 4a, was further used to fabricate hcPSES:PEDOT:PSS-based PV devices. This device structure allowed the p-type hcPSES:PEDOT:PSS layer fully expose to the environment without protection, which intended to perform a rapid evaluation for long term stability of the PV devices. Figure 6 illustrated a typical cross section SEM image of the hcPSES:PEDOT:PSS thin film on our hybrid PV devices, which presented ~ 7.5 μm of the thickness. This film had ~80% transparency and ~200 Ω/□ sheet resistance. An impressive stability was obtained for our hcPSES:PEDOT:PSS PV devices as shown in Figure 7a where J-V characterisation of the hcPSES:PEDOT:PSS PV devices was illustrated. Performance of our hybrid hcPSES:PEDOT:PSS PV devices without encapsulation gradually improved with time after stored under an ambient condition for 140 hours. Performance parameters of the PV devices from J-V curves were listed in Table 3. V_{oc}, FF, and PCE moderately increased from 0.40 to 0.44 (V), 0.46 to 0.49, and 1.92% to 2.32%, respectively while J_{sc} retained within the range of from 10.54 to 10.94 mA/cm^2. PCE enhancement of our PV devices with time may be attributed to formation of a passive SiO_2 film at the interfacial surface between the c-Si substrate and the hcPSES:PEDOT:PSS layer. As a comparison, Figure 7b presented the J-V behaviour of a hcPEDOT:PSS hybrid PV device with the same structure as shown in Figure 4a. A full degradation was observed from J-V characterisation of the hcPEDOT:PSS PV device after stored in air for overnight. The degradation was caused by water trapped or absorbed in the PV devices. Water trapped in the hcPEDOT:PSS layer can lead to a notably abatement of the PV device after stored under an ambient condition for 10 min.[12] Moreover, in order to perform a rapid stability assessment, our hcPSES:PEDOT:PSS hybrid device was then immersed in DI water for another 96 hours after kept in the ambient condition for 140 hr.

In the case of no encapsulation, J-V performance of the hcPSES:PEDOT:PSS hybrid PV device did not degrade as shown in Figure 7a. It still illustrated 2.2% PCE with other parameters listed in Table 3. This superior water-repellent property was attributed to the incorporation of PESE in PEDOT:PSS to form a nanocomposite thin film, which provided a "water-impermeable" property in n-type c-Si hybrid PV devices. This approach in this report could deliver one of the best solutions for manufacturing long term stable and low cost organic-inorganic solar cells and pave the way to realise the true commercial products.

Chemical structures of the hcPSES:PEDOT:PSS and hcPEDOT:PSS thin films were separately characterised by FTIR. Their spectra were presented in Figure 8. For hcPEDOT:PSS thin films, absorption peaks between 3140-2970 cm^{-1} are associated with the stretching vibration of O-H. The absorption peak at 2923 cm^{-1} is related to the alkyl C-H stretching vibration. Peaks at 1646, 1432, and 1413 cm^{-1} are assigned to aromatic -C=C- stretching vibrations. IR bands at 1523, 1294, and 948 cm^{-1} are associated with vibrations of the thiophene ring. Absorption peaks at 1176, 1126, 1091 cm^{-1} are attributed to the stretching vibrations in -C-O-C- ethylenedioxy ring or $-SO_3^-$ asymmetric stretching vibrations. The symmetric stretching vibrations of $-SO_3^-$ are located at 1025 and 1002 cm^{-1}. The O-C-C deformation of the dioxane ring may assign to 900 cm^{-1}. IR spectra of the hcPSES:PEDOT:PSS thin film illustrated significant difference in comparison with that of the hcPEDOT:PSS thin film because of incorporation of polysiloxanes in the structures. IR bands between 1218-966 cm^{-1} are associated with -Si-O-Si- stretching vibrations. Absorption peaks at 1409, 1272, 798, and 769 cm^{-1} are assigned to Si-C-H vibrations in polysiloxanes.

4 Conclusions

A novel, highly transparent and highly conductive nanocomposite thin film was produced at 85^{o}C from a mixture of a sol-gel modified PSES with the aqueous PEDOT:PSS solution. The

PSES has significantly enhanced the water- and scratch- resistance of the PEDOT:PSS thin film with negligible effects on the properties of electrical conductivity when it was used to fabricate n-type c-Si Schottky hybrid PV devices. This could be attributed to a high conductivity of the PSES:PEDOT:PSS nanocomposite thin film along the direction perpendicularly to the surface of the substrate. Due to well-known hydrophobicity of PSES, the PSES:PEDOT:PSS nanocomposite thin film presented a "water-impermeable" property. This behaviour led to the PSES:PEDOT:PSS and c-Si Schottky hybrid PV device with a remarkable stability; i.e. without showing J-V performance degradation even if directly immersed in DI water without protection.

Acknowledgements:

The authors would like to acknowledge in part the financial support from dstl (MoD, UK) under contract number DSTLX 1000085820.

References:

[1] Thiyagu S., Hsueh C-C, Liu C-T, Syu H-J, Lin T-C, & Lin C-F, Nanoscale, 2014, 6, 3361-3366.

[2] Zhang, Y., Zu, F., Lee, Shuit-Tong, Liao, L., Zhao, N., & Sun, B., Adv. Energy Mater. 2014, 4: 1300923. doi: 10.1002/aenm.201300923.

[3] Yu P., Tsai C-Y, Chang J-K, Lai C-C, Chen P-H, Lai Y-C, Tsai P-T, Li M-C, Pan H-T, Huang Y-Y, Wu C-I, Chueh Y-L, Chen S-W, Du C-H, Horng S-F, & Meng H-F, ACS Nano 2013, 7, 10780–10787.

[4] Wei W-R, Tsai M-L, Ho S-T, Tai S-H, Ho C-R, Tsai S-H, Liu C-W, Chung R-J, & He J-H, Nano Lett. 2013,13, 3658–3663.

[5] Chen, J. Y., Yu, M. H., Chang, S. F., & Sun, K. W., Appl. Phys. Lett. 2013, 103, 133901.

[6] He, L., Lai, D.,Wang, H., & Jiang, C. R., Small 2012, 8, 1664–1668.

[7] Jeong S., Garnett E. C., Wang S., Yu Z., Fan S, Brongersma M. L., McGehee M. D., Cui Y., Nano Lett. 2012, 12, 2971–2976.

[8] Liu, Q., Ono, M., Tang, Z., Ishikawa, R., & Ueno, K., Appl. Phys. Lett. 2012, 100, 18390.

[9] Zhang Y; Cui W., Zhu Y, Zu F, Liao L, Lee S, Sun B, Energy Environ. Sci., 2014, DOI: 10.1039/C4EE02282C.

[10] Lam C. Y., Shi S. Q., Lu J., & Chan P. K. L., Proceed-ings of the ASME 2013, ES2013-18265, 7th International Conference on Energy Sustainability, Minneapolis, MN, USA. 2013, July 14-19.

[11] Schmidt J., Titova V., & Zielke D., Appl. Phys. Lett. 2013, 103, 183901.

[12] He W. W., Wu K. J., Wang K., Shi T. F., Wu L., Li S. X., Teng D. Y., & Ye C. H., 2014, 4, 3715; DOI:10.1038/srep03715.

[13] Elschner A., Kirchmeyer S., Lovenich W., Merker U., & Reuter K., CRC Press, ISBN 1420069128, 9781420069129, 2010, 167-242.

[14] Groenendaal L., Jonas F., Freitag D., Pielartzik H., Reynolds J. R., Adv. Mater. 2000, 12, 481-494.

[15] Kim YS, Oh SB, Park JH, Cho MS, Lee Y, Sol. Energy Mater. Sol. Cells 2010, 94 , 471–477.

[16] Somboonsub B, Invernale MA, Thongyai S, Praserthdam P, Scola DA, Sotzing GA, Polymer 2010, 51, 1231–1236.

[17] Po R., Carbonera C., Bernardi A., Tinti F., & Camaioni N., Sol. Energy Mater. Sol. Cells 2012, 100, 97–114.

[18] Liu C, Jiang F, Huang M, Yue R, Lu B, Xu J, and Liu G, J Electronic Mater. 2011, 40, 648-651.

[19] Y. Xia, K. Sun and J. Ouyang, Adv. Mater., 2012, 24, 2436-2440.

Figure 1 Schematic diagram for microstructures of the PSES:PEDOT:PSS nanocomposite thin films where one could travel from A to A' or B to B' in its same phase. The arrow starting in the PEDOT:PSS phase (C point) and entering perpendicularly into the nearest PSES surface must re-emerge in another PEDOT:PSS phase within nanometres away. Conversely, the arrow originating in the PSES phase (D point) and passing perpendicularly into the nearest PEDOT:PSS surface will re-emerge in another PSES phase.

Figure 2 (a) Backscattered SEM images of a six-layer spin-coated PSES:PEDOT:PSS film from SGP-1 and SEM- EDX elemental of Si mapping on the bottom left and C mapping on the bottom right; (b) SEM morphologies of the PSES:PEDOT:PSS nanocomposite thin film; (c) AFM morphologies of the PSES:PEDOT:PSS nanocomposite thin film (the height bar is 30 nm and the scale of images is 2 μm x 2 μm).

Figure 3 (a) Transmittance and sheet resistance of PSES:PEDOT:PSS thin films on PP from SGP-1; Sample A is one-layer-film with ~4-μm-thickness; Sample B is three-layer-film with ~12-μm-thickness; and sample C is six-layer-film with ~24-μm-thickness. (b) Relationship of sheet resistance and transmittance of hcPESE:PEDOT:PSS thin films from SGP-2; (c) Transmittance and sheet resistance of PSES:PEDOT:PSS thin films on PP after adding Ag nanowires.

Figure 4 (a) Schematic diagram of structures of PSES:PEDOT:PSS nanocomposite or PEDOT:PSS PV devices; (b) J-V characterisation of hybrid PV devices fabricated by the PEDOT:PSS aqueous solution and PSES:PEDOT:PSS solution with the structure as shown in (a), respectively.

Figure 5 (a) Schematic diagram of structures of hcPSES:PEDOT:PSS nanocomposite or hcPEDOT:PSS PV devices; (b) J-V characterisation of hybrid PV devices fabricated by the

hcPEDOT:PSS aqueous solution and hcPSES:PEDOT:PSS with the structure as shown in (a), respectively.

Figure 6 SEM cross section images of hcPSES:PEDOT:PSS thin films for the hybrid PV devices, showing ~ 7.5 μm thickness.

Figure 7 (a) Stability performance of J-V characterisation of the hcPSES:PEDOT:PSS nanocomposite PV devices with the structure as shown in Figure 4a; (b) Degradation of J-V behaviour of hcPEDOT:PSS hybrid PV devices with the structure as shown in Figure 4a.

Figure 8 FTIR spectra of the hcPSES:PEDOT:PSS and hcPEDOT:PSS thin films which were cured at 120^{o}C for 10 min.

Figure 1 Schematic diagram for microstructures of the PSES:PEDOT:PSS nanocomposite thin films where one could travel from A to A' or B to B' in its same phase. The arrow starting in the PEDOT:PSS phase (C point) and entering perpendicularly into the nearest PSES surface must re-emerge in another PEDOT:PSS phase within nanometres away. Conversely, the arrow originating in the PSES phase (D point) and passing perpendicularly into the nearest PEDOT:PSS surface will re-emerge in another PSES phase.

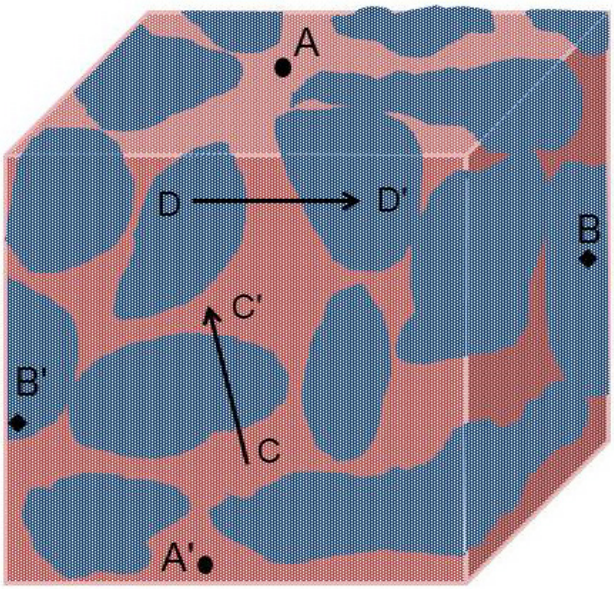

Figure 2 (a) Backscattered SEM images of a six-layer spin-coated PSES:PEDOT:PSS film from SGP-1 and SEM- EDX elemental of Si mapping on the bottom left and C mapping on the bottom right; (b) SEM morphologies of the PSES:PEDOT:PSS nanocomposite thin film; (c) AFM morphologies of the PSES:PEDOT:PSS nanocomposite thin film (the height bar is 30 nm and the scale of images is 2 µm x 2 µm).

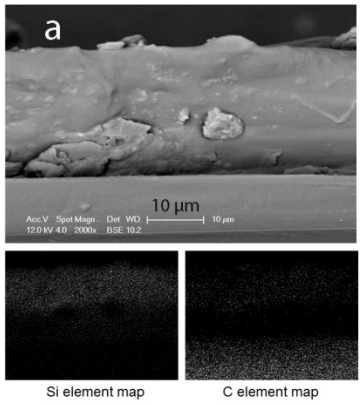

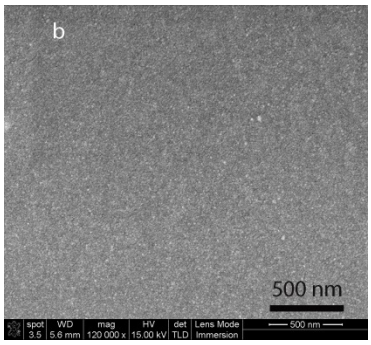

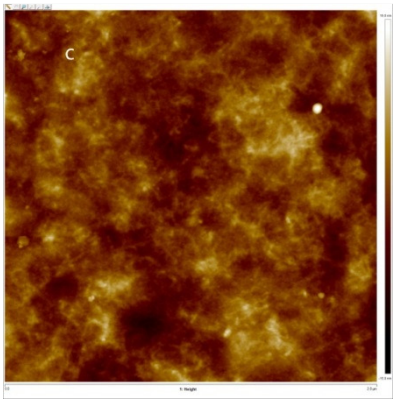

Figure 3 (a) Transmittance and sheet resistance of PSES:PEDOT:PSS thin films on PP from SGP-1; Sample A is one-layer-film with ~4-μm-thickness; Sample B is three-layer-film with ~12-μm-thickness; and sample C is six-layer-film with ~24-μm-thickness. (b) Relationship of sheet resistance and transmittance of hcPESE:PEDOT:PSS thin films from SGP-2; (c) Transmittance and sheet resistance of PSES:PEDOT:PSS thin films on PP after adding Ag nanowires.

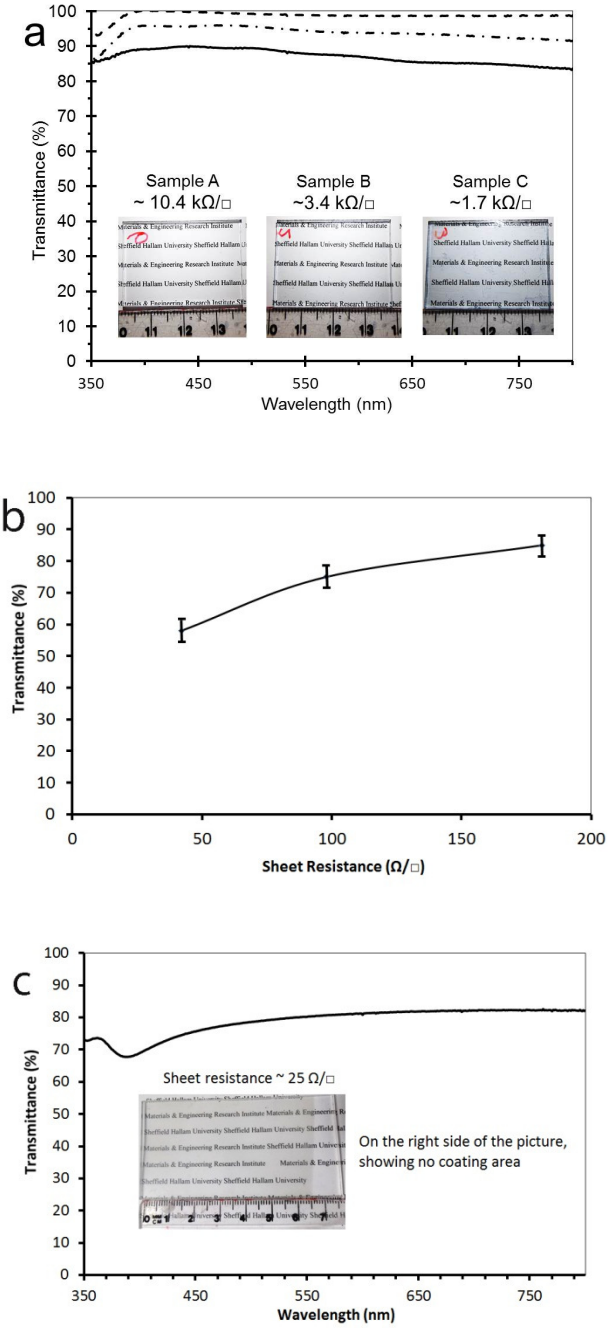

Figure 4 (a) Schematic diagram of structures of PSES:PEDOT:PSS nanocomposite or PEDOT:PSS PV devices; (b) J-V characterisation of hybrid PV devices fabricated by the PEDOT:PSS aqueous solution and PSES:PEDOT:PSS solution with the structure as shown in (a), respectively.

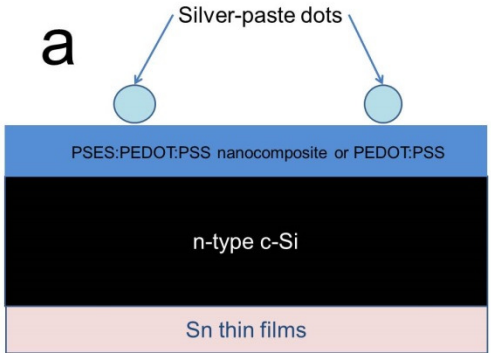

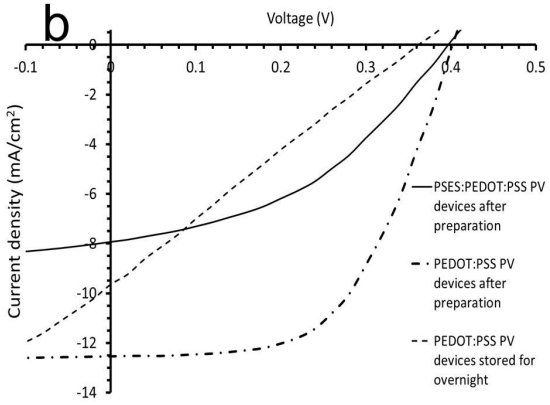

Figure 5 (a) Schematic diagram of structures of hcPSES:PEDOT:PSS nanocomposite or hcPEDOT:PSS PV devices; (b) J-V characterisation of hybrid PV devices fabricated by the hcPEDOT:PSS aqueous solution and hcPSES:PEDOT:PSS with the structure as shown in (a), respectively.

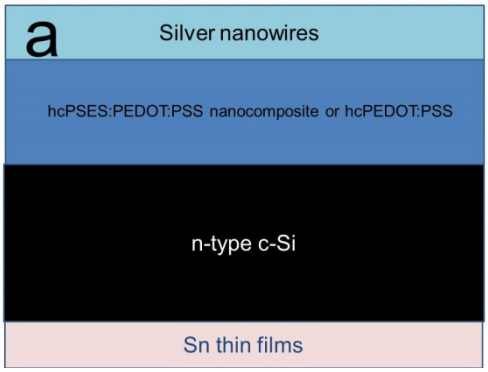

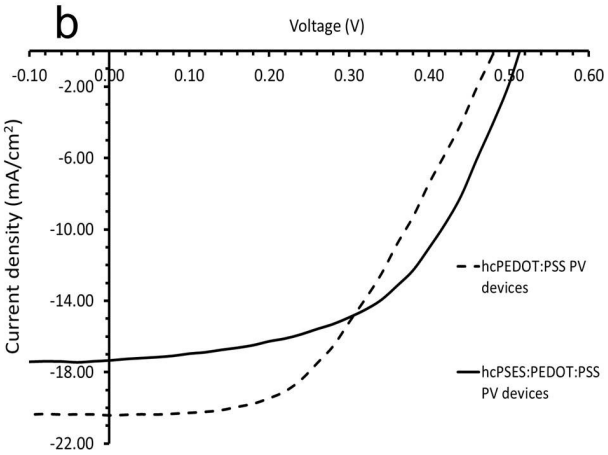

Figure 6 SEM cross section images of hcPSES:PEDOT:PSS thin films for the hybrid PV devices, showing ~ 7.5 μm thickness.

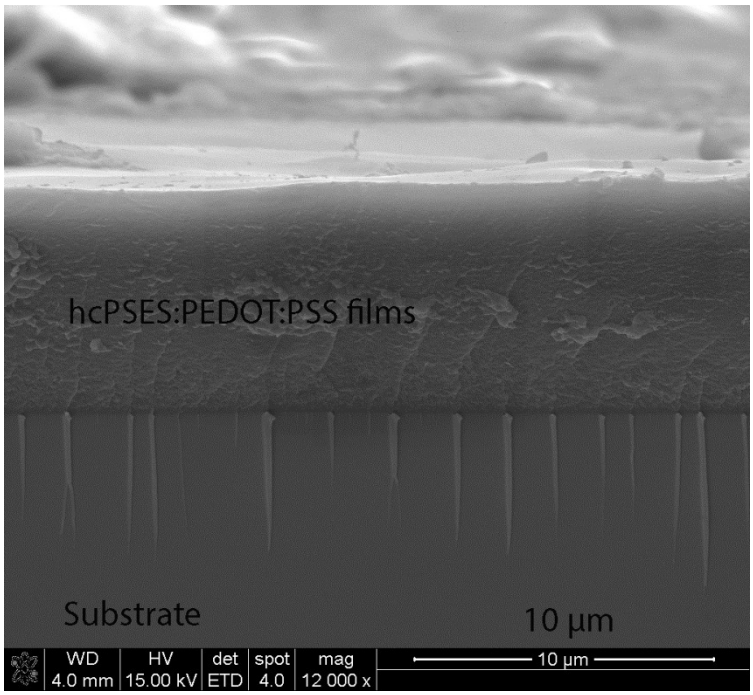

Figure 7 (a) Stability performance of J-V characterisation of the hcPSES:PEDOT:PSS nanocomposite PV devices with the structure as shown in Figure 4a; (b) Degradation of J-V behaviour of hcPEDOT:PSS hybrid PV devices with the structure as shown in Figure 4a.

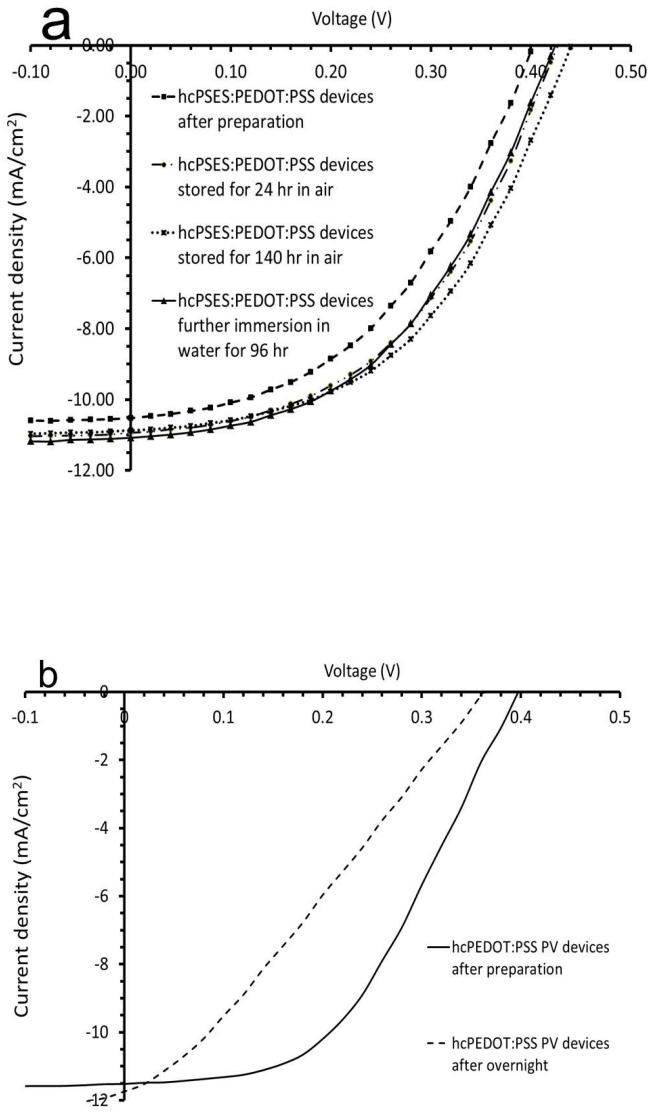

Figure 8 FTIR spectra of the hcPSES:PEDOT:PSS and hcPEDOT:PSS thin films which were cured at 120^{o}C for 10 min.